JET IMPACT FACILITY FOR DIRECT MEASUREMENT OF MOMENTUM

P. George Oommen

A DISSERTATION

in

The Faculty

of

Engineering

Presented in Partial Fulfillment of the Requirements for
the Degree of Master of Engineering
Concordia University
Sir George Williams Campus
Montreal, Canada.

October 1974.

ABSTRACT

P. GEORGE OOMMEN

JET IMPACT FACILITY FOR DIRECT MEASUREMENT OF MOMENTUM

The momentum distribution in a manifold is an important factor in the design of effluent disposal systems. In the present study, the effect of jet spacing ratio and jet area ratio on the momentum distribution along the length of a manifold are investigated. A general equation including jet area, jet spacing and length of a manifold is obtained. To verify the theoretical model a jet impact tank was developed. Results indicate that the theoretical model is valid for short pipes in which friction can be neglected.

ACKNOWLEDGEMENT

The author wishes to thank Dr. A.S. Ramamurthy for suggesting the development project related to the jet impact facility for direct measurement of momentum. Numerous discussions and valuable help given by Dr. Luc Robillard and Dr. Subramanya are very much appreciated.

The assistance of Mr. L. Stinkebizius of the Environmental Fluid Mechanics Laboratory is thankfully acknowledged.

TABLE OF CONTENTS

List of Tables iv

List of Figures v

List of Symbols vi

Introduction 1

Previous Work 3

Some Theoretical Considerations 7

Experimental Studies 10

Discussion of Results 13

Summary and Conclusion 17

Scope for Further Work 18

Appendix A: - Experimental Data 39

Appendix B: - Specimen Calculation 44

References 47

LIST OF FIGURES

		Page
Figure 1.	Schematic layout of experimental set up.	25
2.	Retainere and manifold	26
3a	Test tank	27
3b	Test tank (photograph)	28
3c	Test tank (photograph)	
4.	Momentum balance	29
5.	h computed vs h observed	30
6.	Q computed vs Q observed	31
7.	Momentum measured using balance vs momentum measured using pitot-tube	32
8.	Theoretical momentum distribution	33
9.	Momentum distribution, $A_r = 0.35$	34
10.	Momentum distribution, $A_r = 0.17$	35
11.	Momentum distribution, $A_r = 2.73$	36
12.	Momentum distribution, $A_r = 0.17$	37
13.	Momentum distribution, $A_r = 0.35$	38

LIST OF TABLES

		Page
Table 1.	An abstract of review of literature for lateral out flow in perforated pipes.	19
2.	Tube geometry.	21
3.	Measured and theoretical static Head.	22
4.	Theoretical and Measured discharges.	23
5.	Momentum measured by using pitot-tube and the balance.	24

LIST OF SYMBOLS

A	Cross sectional area of manifold
A_r	Area ratio, a/A
a	Total area of jet per unit length
D	Inside Diameter of manifold
d	Diameter of jet
f	Coefficient of friction
g	Acceleration due to gravity
H	Total head
h	Static head
h_f	Head loss due to friction
L	Active length of pipe
M_o	Momentum at S = 0
M_s	Momentum at any section
M_r	Momentum ratio
P	Pressure
Q	Total discharge
q	Discharge from unit length of pipe
s	Distance from dead end of manifold
V	Longitudinal velocity in pipe
V_1	Velocity of discharge from pipe
k	a constant
ρ	density
α	Correction factor
μ	Discharge coefficient of jet = 0.61

CHAPTER 1

INTRODUCTION

CHAPTER 1

INTRODUCTION

Recently, engineers are more and more concerned about better ways of disposing industrial and municipal wastes into streams. One of the design requirements is to discharge the effluent uniformly along the width of the stream.

Usually, these systems discharging the effluent include a manifold i.e. multiport pipes (Fig. 1b) as part of the system. When the effluent is discharged into a body of water as a counter-flowing or co-flowing jet, the discharge from the individual orifice may act as independent jets in the vicinity of the jet exit plane. It has been demonstrated that the momentum of the jet is an important parameter that controls the mixing characteristics of a counter jet. A very non-uniform distribution of the effluent discharge along the pipe may inhibit the formation of a quasi two-dimensional jet. In fact, the individual jets may not coalise and act in unison. This will reduce the efficiency of mixing in the counter jet. As such, the momentum distribution from the multiport outlets has significant bearing in the design of these systems.

In this project, the effect of jet spacing and area on the momentum distribution along the length of the pipe has been studied. Experimental study on the momentum distribution by using pipes with different diameters and different spacing is reported. The study was preceded by a development relating to the design and fabrication of a jet impact facility.

Theoretical study conducted by Noseda (1) on horizontal pipes with uniformly distributed holes is found to be useful for preliminary design calculations. The present investigation provides some verification of this theory and provides an indication about the ranges where the theory is applicable.

The problem treated presently finds many field applications. For instance, manifolds are used in the following:

1) Canal lock manifolds (time of filling and emptying)
2) Thermal discharge diffusers
3) Sewage disposal
4) Sprinkler irrigation systems
5) Water filtering systems
6) Oil burner design
7) Fluid lines with distributed leakage
8) Bio engineering systems

CHAPTER II

PREVIOUS WORK

CHAPTER II

PREVIOUS WORK

During the past, many attempts have been made to solve manifold problems. A summary of some of the important contributions to the manifold problem is given below.

In a comprehensive paper, Keller (2) deals with the case of a manifold supplying the fluid to a set of parallel pipes or ducts discharging through a number of orifices distributed along the manifold lengths. He systemized the problem as follows:

1) Single pipe or duct, with lateral discharge openings
2) Single manifold, feeding a multitube grid of pipes
3) Inlet manifold and discharge manifold, connected by a multitube grid of pipes

In order to solve the problem, in general, he obtained a differential equation for the velocity from the basic equations of motion. For the case of flow through a manifold shown in fig. 3d.

Pressure rise in the direction of flow in the manifold is

$$\frac{dp}{\rho} = \left[\frac{d(V^2)}{2}\right] + f\frac{(ds)}{D}V^2 \qquad (1)$$

When the manifold cross section is uniform and the openings are uniformly distributed; the following relations hold true.

$$dq = AdV = K V_1 (ads) \qquad (2)$$

$$\text{But } V_1 = \sqrt{2g \cdot \frac{P}{\gamma}} \qquad (3)$$

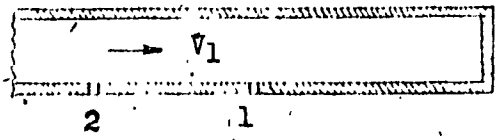

Fig. 3.d

Using the above relations, Keller obtained the following relation.

$$\left(\frac{A}{Ka}\right)^2 \left(\frac{d^2V}{dS^2}\right) = -V \left(\frac{fg}{D}\right) \frac{V^2}{dV/ds} \qquad (4)$$

which is a second order differential equation for which no exact solution can be found.

Keller (2) showed that the discharge profile was essentially determined by the relative value of the pressure regain arising from deceleration and by the pressure loss caused by the friction. Keller dealt with the problem without considering the state of flow, the rate of discharge, variation in Reynolds number and pressure loss due to branching.

Noseda (1) has given some experimental data for flow through a perforated pipe. His theoretical results for frictionless flow are essentially the same as the results of Keller.

While studying the canal lock filling system, Allen and Albinson (3) suggested a different less rigidly formulated approach to obtain uniform discharge through the ports along the length of the culverts. In this paper they suggested a step by step method

for the design of the ports and obtained a satisfactory measure of agreement between theory and experiments.

Olson (4) investigated the case of a long pipe of uniform cross sectional area with uniformly porous wall and determined the differential equations connecting the rate of flow to the pressure drop in the pipe. Since he neglected the kinetic energy term, the solution is valid only for the limiting case of small discharge.

Vigander and Brooks (5) described a model study from which the discharge coefficient was obtained for lateral flow through a corrugated pipe. Tests were made for various hole sizes and number of holes in axial and circumferential direction. They also described a method used to compute the pipe diameter and hole configuration necessary to obtain uniform spatial distribution of discharges for a given flow rate and head. A description of a thermal diffuser system is also included in the paper.

Berlamont and Van der Bekin (6) suggested a general solution for obtaining a uniform lateral out flow, either by varying the perforation area or the pipe cross sectional area. The distribution of the lateral out flow in a conduit with constant cross section and constant perforation area is analysed in a normalized form. In this analysis pressure recovery, velocity distribution effect and laminar and turbulent flow parameters have been included. The comparison between

the experimental values and calculated values are very close. A properly chosen velocity correlation coefficient can give satisfactory results.

Table 1, gives an abstract of review of literature for lateral outflow in perforated pipes.

CHAPTER III

SOME THEORETICAL CONSIDERATIONS

CHAPTER III

SOME THEORETICAL CONSIDERATIONS

Figure 1b is a definition sketch of lateral flow through a perforated pipe.

Consider a steady flow of a newtonian incompressible fluid in a horizontal pipe with uniformly spaced holes with its efflux into a body of same fluid of constant head

$$\frac{dh}{ds} + \frac{d}{ds}\left(\alpha \frac{V^2}{2g}\right) + \frac{dh_f}{ds} = 0 \qquad (6)$$

Assuming completely no loss conditions, $h_f = 0$

$$\frac{dh}{ds} + \frac{d}{ds}\left(\alpha \frac{V^2}{2g}\right) = 0$$

Since $V = \frac{q}{A}$,

$$\frac{dh}{ds} + \alpha \frac{q}{A^2} \cdot \frac{dq}{ds} = 0 \qquad (7)$$

The discharge from unit length of the pipe is given by the equation

$$Q_s = \frac{dq}{ds} = \mu a\sqrt{gh} \qquad (8)$$

where μ = coefficient of discharge

a = total area of jet per unit length

h = piezometric head

s = distance from the dead end of the manifold

L = length of the manifold

Solving equation (8) for h, we get

$$\frac{dh}{ds} = \frac{1}{g\mu^2 a^2} \cdot \frac{dq}{ds} \cdot \frac{d^2q}{ds^2} \qquad (9)$$

substituting equation (9) in equation (7) we have

$$\frac{d^2q}{ds} + \alpha \left(\frac{\mu a}{A}\right) q = 0 \qquad (10)$$

This is the basic differential equation for the lateral out flow. Using this equation Noseda (1) obtained the expression for piezometric head as

$$h = H \cos^2 x \sqrt{\alpha}$$

where H the total head and $x = \frac{\mu a s}{A}$

$$h = H \cos \frac{\mu a s}{A} \qquad (11)$$

The momentum at any point can be defined as

$$M_s = \rho Q_s V_s$$

$$M_s = \rho \cdot \frac{Q_s^2}{a^2} \qquad (12)$$

substituting equation (8) in equation (12)

$$M_s = \frac{\rho \mu^2 a^2 2gh}{a}$$

$$= \rho \mu^2 a \cdot 2gh \qquad (13)$$

Substituting equation (11) in equation (13),

$$M_s = \rho \mu^2 a \, 2gH \cos^2 \frac{\mu a}{A} s$$

$$= \rho \mu^2 \, 2gH \cos^2 \frac{\mu a}{A} L \cdot \frac{s}{L}$$

Boundary Conditions at $S = 0$, $h = h_o$, $q_o = \mu a_o \sqrt{2gh}$, $Q = Q_o$

$S = L$, $L_L = h_o + \frac{Q_o^2}{A^2 2g}$, $q_L = \mu a_L \sqrt{2gh_L}$, $Q = o$

$$M_o = \rho \mu^2 a \, 2gH \, \text{Cos}^2 (\frac{\mu a}{A} \cdot 0)$$

$$M_o = \rho \mu^2 a \, 2gH$$

$$\frac{M_s}{M_o} = \text{Cos}^2 (\mu \frac{a}{A} L \cdot \frac{S}{L}) \qquad (14)$$

$$\frac{M_s}{M_o} = M_r = \text{Cos}^2 (K \frac{S}{L}) \qquad (15)$$

where $K = \frac{\mu a}{A} \cdot L$

Equation (15) gives the momentum distribution in a normalized form for the perforated frictionless pipe: M_r for different a/A are plotted in figure (8).

An experimental investigation was conducted to obtain the information on the effect of area ratio, spacing etc. on the momentum distribution and to evaluate the theoretical model. The experimental work is reported in the following chapters.

CHAPTER IV

EXPERIMENTAL STUDIES

Chapter IV

EXPERIMENTAL STUDIES

Experimental Set Up

The schematic sketch for the experimental set up is shown in figure 1a. The set up essentially consists of:

1) manifold tube
2) test tank
3) momentum balance
4) flow measuring devices

i) The manifold tube

The tubes were of solid drawn smooth brass with one row of holes of uniform size and spacing drilled along the length. The tube geometry is given in table 2. The ends of the test tube were connected to two equal high pressure flexible hoses, with the help of proper adapters, which in turn were connected to the main supply line through a control valve and an orifice meter. A valve was connected at one end of the hose to block the flow. The injection devices are shown in figure 1a. The manifold was installed in the test tank with the help of a pair of retainers (figure 2). The alignement of the manifolds could be adjusted with the help of a pair of bolts on the top of the retainers.

ii) The Test Tank

The test tank (figures 3a, 3b, 3c) was 48" wide and 36" long. A baffle wall 2' high was used near the outlet to maintain a constant head in the tank. The test tank and the baffle walls were made of transparent 1/2" thick plexi glass. The tank was reinforced by angles around to prevent

possible buckling. As shown in figure 3a, a beam (1" x 1" angle) and 1/8" thick steel platform were installed on the top of the tank to secure the momentum balance, retainer and the pitot tube mountings. The whole set up was mounted on a steel platform with casters for easy manoeuverability.

iii) Momentum Balance

Lin (7) in his studies on counter jet, used a balance type device to measure momentum; using the same principle, a larger sensitive momentum balance was fabricated for measuring the total momentum for the present studies.

The balance (figure 4) used for tests was made of aluminum. A disk was attached to one end of the horizontal arm and a rider was attached to the other end to compensate for any ititial unbalanced conditions. The jet impinging plate made of aluminum was attached to the vertical leg.

In the tests, the displacement of the plate due to the jet impingement was counter balanced by using the weights on the pan and the momentum was read directly.

Flow Measuring

i). The total flow was measured by a standard orifice meter set in a 2' main line. The orifice meter was installed ten feet away from the main valve and eight feet from the control valve.

ii) The velocity profile due to jets were measured by a pitot tube. An inclined manometer capable of reading up to 0.002 inches was

used to measure the velocity head .

iii) The entrance pressure was measured using two systems. Pressures less than 2 psi were measured using a pizometer and higher pressures were measured using a standard pressure gauge.

Test Procedure

The tank was levelled before each test. The orientation of the jet was checked by observing the free flow of water through the perforation. Adjustments to the alignment of the pipe were made to keep the pipe horizontal. Before starting any tests, trapped air from the system was completely bleeded out.

In a typical test, the outlet valve was regulated to get the desired flow conditions (two way or one way flow); a known discharge was passed through the system. The velocity profile was traced in a grid of 0.2 inches vertical spacing and 1.33 inches horizontal spacing.

The orifice meter readings and the inlet pressures were recorded.

The momentum balance was used to find the total momentum. Appendix A gives the summary of data from various tests.

CHAPTER V

DISCUSSION OF RESULTS

CHAPTER V

DISCUSSION OF RESULTS

Since the frictionless model was derived assuming no loss conditions, it is essential to verify its validity of the proposed model. Some preliminary computations were done for this purpose to cover the following aspects.

i) Comparison of measured static head and theoretical static head.

As explained in Chapter Iv, the entrance pressure was measured directly at the entrance. Since an adapter was used at the entrance, the pressure at the adapter is converted to actual entrance pressure using Bernoullis' equations. (See Appendix B)

The theoretical entrance pressure is computed using the equation.

$$\frac{h}{H} = \text{Cos} \quad \frac{\mu as}{A} \qquad (11)$$

The results are tabulated in Table 3. A graph (figure 5) is plotted using h computed vs h observed as the variables. The results appeared to be very satisfactory.

ii) Comparison of the total discharge measured and computed:-

The validity of the model was also verified using one of Noseda's (1) equations for the rate of flow.

$$Q = A\sqrt{\frac{2gH}{\alpha}} \quad \mathrm{Sin}\left(\frac{\mu a}{A} L.\alpha\right) \qquad (16)$$

Assuming $\alpha=1$, Q was computed using equation (16) and compared with the actual discharges. Actual discharge and computed discharges are tabulated in Table 4. The results are plotted in figure 6. The results are satisfactory.

In view of the above results the validity of the mathematical model for short pipes in which friction can be negligible is established.

Momentum Studies

The momentum at any section may be defined as $\int \rho\, v^2 ds$ which is the area under the $v^2/2g$ curve. As described in the previous section, the velocity profile was measured using the pitot tube. The area under the curve is calculated assuming linear variation of momentum. Actual momentum of each position is computed using a simple computer program.

In this project four different manifolds of different a/A ratios were used. A total of twenty three sets of velocity traverse were recorded using the above manifolds for different discharges. Because of the high sensitivity of the inclined manometer, the velocity distribution could be measured very accurately. Data and results of five sets of velocity traverse are given in Appendix A.

A check on the integrated value of momentum was obtained by measuring the direct jet impact on the balance. Total momentum was measured for all the twenty three above cases. The balance used for the tests was capable of measuring 0.5 gms and maximum range was about ten pounds. The total momentum measured using the pitot tube and the balance, is tabulated in Table 5 and the results are plotted in figure 7. An enveloping curve is also drawn (figure 7) to find the deviation from the expected results. The maximum deviation in the result is only 5%. In general the momentum measured by the balance agrees fairly well with the momentum graphically estimated.

THEORETICAL MOMENTUM DISTRIBUTION

To study the effects of jet area and spacing on the distribution of momentum along the length of a manifold a non-dimensional equation is derived. (equation 15)

i.e. $M_r = \frac{Ms}{Mo} = \cos^2\left(K.\frac{S}{L}\right)$ This equation is plotted in figure 8. The results show that, in general, the momentum distribution is almost uniform for smaller values of a/A. As a/A increases the momentum distribution becomes more and more non-uniform. Since a negative momentum distribution is not possible, the mathematical model is not satisfactory for values of $\left(K.\frac{S}{L}\right) > \frac{\pi}{2}$

EXPERIMENTAL RESULTS

Two typical examples of actual momentum distribution (one way flow) along the length of the manifold with an area ratio of 0.35 and 0.17 are plotted in figures 9 and 10. The momentum distribution is more scattered in the first case than in the second one. This is due to the fact that as area ratio decreases the momentum distribution

becomes more and more uniform. The theoretical momentum distribution of manifolds whose a/A ratios are 0.35 and 0.17 are also shown in figures 9 and 10 respectively. Comparison between the experimental data and the theoretical curve substantiates the validity of the theoretical approach chosen.

As mentioned before, the mathematical model is not satisfactory for values of a/A in excess of 16. This could be seen in figure 11, which is a typical example. In this a/A ratio is 2.8. Figures 12 and 13 are two typical momentum distributions along the length of the manifold for "two way flow". The theoretical curve is plotted by assuming a single "two way" manifold as two "one way" manifolds. The results are found to be satisfactory. In general, the momentum distribution of "two way flows" is more uniform than that of "one way flow".

SUMMARY AND CONCLUSIONS

The present study deals with the effect of area ratio Ar and spacing ratio S/L of jets on the momentum distribution along the length of the manifold. A mathematical model is derived assuming no loss conditions for a short pipe with uniformly spaced holes. Experiments were carried out in order to verify the theory. To this end, a jet impact tank housing a balance to measure the jet momentum was developed. This equipment was tested and found to provide a simple means of verifying the theoretical model for the manifold.

Fairly uniform momentum distribution could be obtained for pipes whose ratios are small. ($A_r \simeq 0.2$) The momentum distribution for "two way flow" is more uniform than that of "one way flow".

During the experimental investigation, the momentum was measured by two methods: (a) using the pitot tube (b) using the momentum balance. The momentum measurement using the pitot tube is a tedious procedure. The momentum balance that has been developed measures the total momentum fairly accurately and the procedure is simple.

SCOPE FOR FURTHER WORK

The main objective of this study was to find the effect of jet area and spacing on the momentum distribution along the length of a manifold. This study was conducted assuming no loss conditions. Further studies are recommended in the following areas:

1- Development of a model incorporating friction for long pipes,

2- Measurements of momentum distribution with various types of flow and boundary conditions,

3- Momentum studies using manifolds of varying geometry.

TABLE 1*

AN ABSTRACT OF REVIEW OF LITRATURE FOR LATERAL OUT FLOW IN PERFORATED PIPES.

AUTHOR	INERTIA	PIPE FLOW	OUTFLOW	SOLUTION
Keller (2)	Included	Turbulent	Turbulent	Step by Step
Allen and Albimson (3)	Included	Turbulent	Turbulent	Step by Step
Olson (4)	Neglected	Laminar	Turbulent laminar	Analytical
Berlamont and Van Der Berkent (6)	Included	laminar turbulent- smooth and rough	laminar or turbulent	Analytical and numerical
Enger and Levy (8)	Included	friction neglicted	Turbulent	Analytical
Dow (9)	Included	laminar turbulent smooth and rough	-	Analytical for variable cross section
Van der Hegge Zijmen (10)	Included	laminar turbulent smooth and rough	laminar or turbulent	Analytical
Howland (11)	Included	Turbulent rough	Turbulent	Step by Step for variable perforation area
Horlock (12)	Included	Turbulent rough	Turbulent	Analytical
Acrivos etc. (13)	Included	Turbulent Smooth	Turbulent	Numerical
Markland (14)	Included	Turbulent rough	Turbulent	Numerical

* after Berlamont (6)

Steel and Shove (15)	Included	Turbulent rough	Turbulent	Numerical
Camp and Giraber (16)	Included	Turbulent rough	Turbulent	Analytical
Vigander etc. (5)	Included	Turbulent rough	Turbulent	Step by Step
Zsak (17)	Neglected	Turbulent rough	Turbulent	Analytical

TABLE 2

TUBE GEOMETRY

Inside Dia of Pipe D inches	Dia. of Jet d 1 inche	spacing inches	No. of holes per foot n	length of pipe L inches	area ratio a/A
0.31	0.052	0.125	96	20	2.80
0.748	0.063	0.25	48	20	0.35
0.748	0.063	0.50	24	20	0.17
1.562	0.120	1.00	12	20	0.07

TABLE NO. 3

MEASURED AND THEORETICAL STATIC HEAD.

Test No. No.	a/A	Cos k	H	h Theoritical	h Measured
15	0.3406	0.8848	7.70	6.81	6.68
16			9.16	8.10	7.51
20			12.75	11.28	10.74
22	0.1703	0.9703	20.11	19.53	19.09
			28.46	27.62	26.82
			38.62	37.48	36.58
52	0.0707	0.9948	23.21	23.09	23.07
14	0.3406	0.8848	6.14	5.34	5.88
17			9.26	8.19	8.85
19			12.96	11.47	12.45
21	0.1703	0.9703	24.06	23.35	23.80
23			34.56	33.53	34.15
25			44.47	43.15	43.96
57	0.0707	0.9948	20.83	20.72	20.77
60	0.1414	0.9795	12.16	11.91	12.10

TABLE NO. 4

THEORITICAL AND MEASURED DISCHARGES

Test No.	Q Measured	Q Theoretical
15	25.1	23.1
16	31.4	28.0
20	35.0	32.7
22	25.1	21.2
24	31.4	26.9
26	35.0	27.5
52	52.3	48.7
14	25.1	20.58
17	31.4	24.96
19	35.0	30.00
21	25.1	22.07
23	31.4	24.64
25	35.0	28.6
57	52.3	38.42
60	52.3	46.3

TABLE NO 5

MOMENTUM MEASURED BY USING PITOT TUBE AND THE BALANCE

Test No.	MP (lbs)	MB (lbs)
3	0.40	0.37
4	0.58	0.54
5	0.96	0.78
8	0.53	0.45
9	0.70	0.67
10	1.23	1.09
14	2.32	1.96
15	2.46	2.12
16	4.01	3.35
17	4.33	3.77
20	5.02	4.84
22	4.61	4.05
23	6.64	6.30
24	6.25	5.63
25	7.62	6.72
26	7.84	7.23
52	8.84	8.22
57	8.52	7.68
60	4.95	4.08

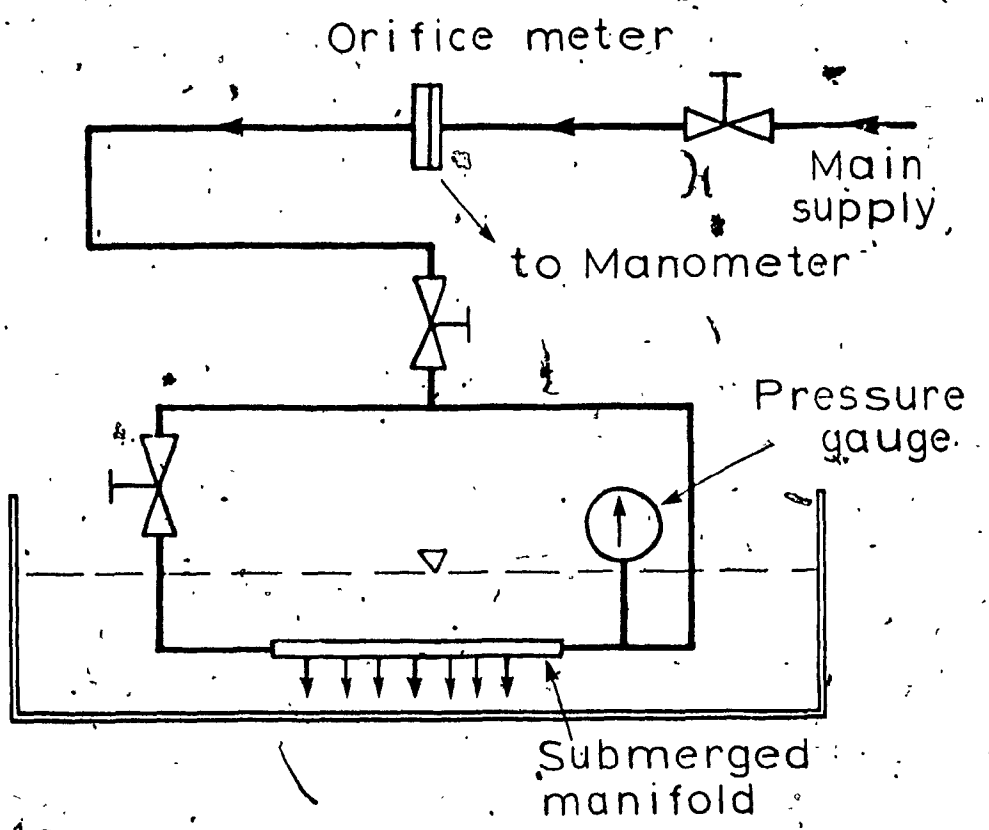

FIG. 1a
SCHEMATIC LAYOUT OF EXPERIMENTAL SET UP

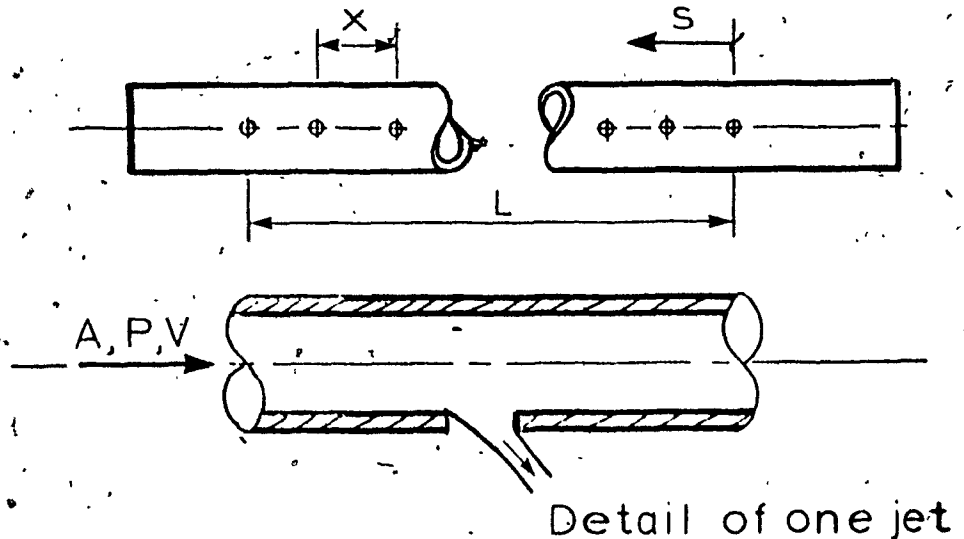

FIG. 1b
MANIFOLD

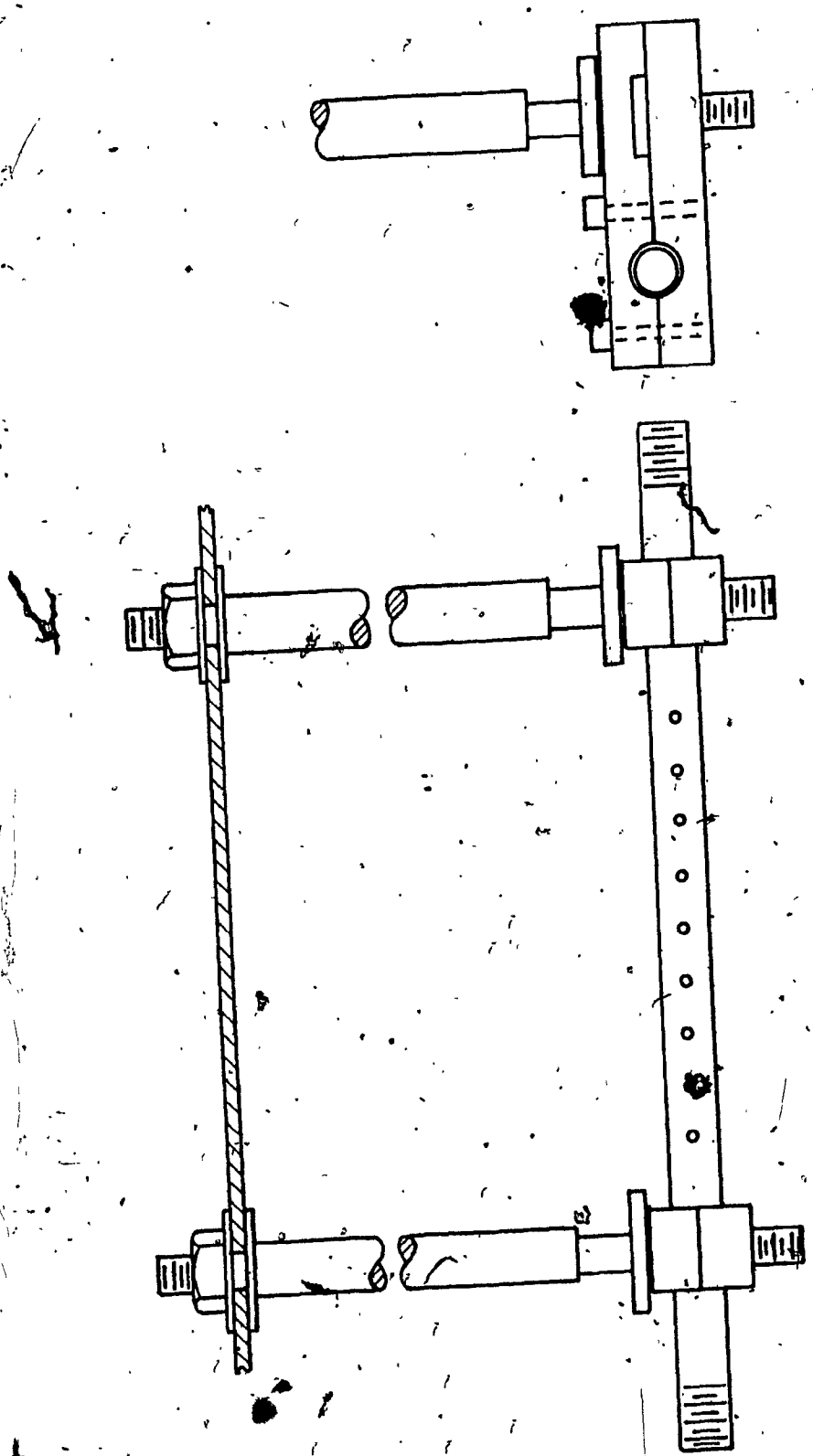

FIG. 2
RETAINERS AND MANIFOLD

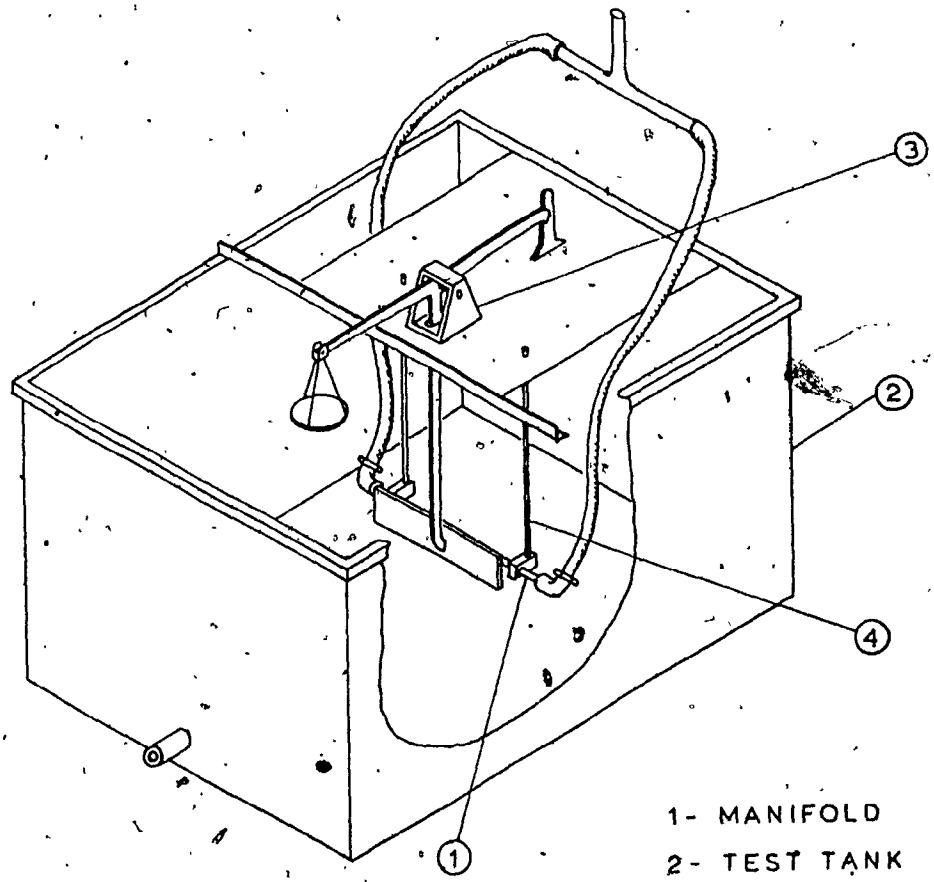

1- MANIFOLD
2- TEST TANK
3- BALANCE
4- RETAINERS

FIG. 3
TEST TANK

Figure 3b
Test tank

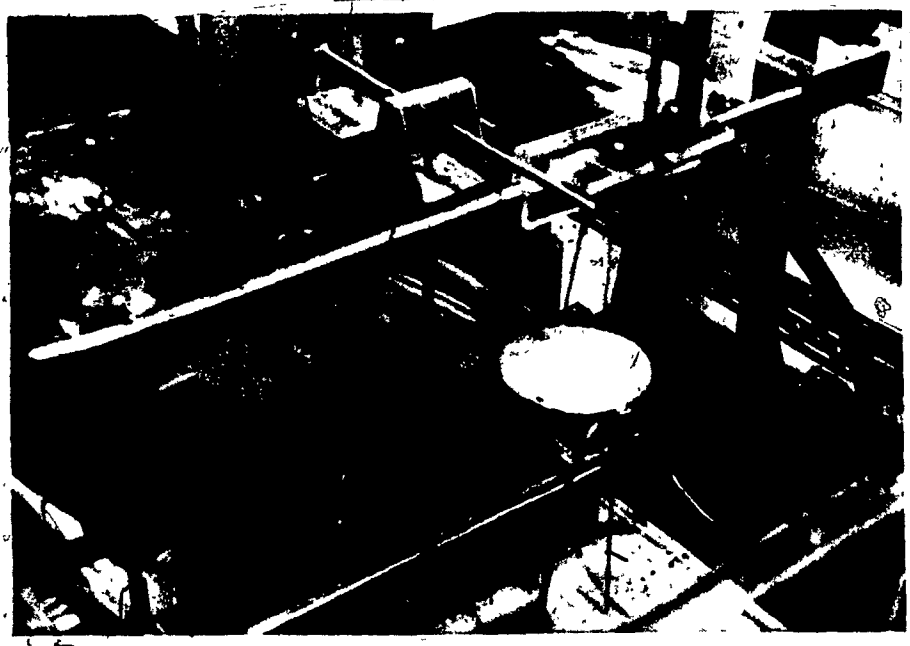

Figure 3c
Test Tank

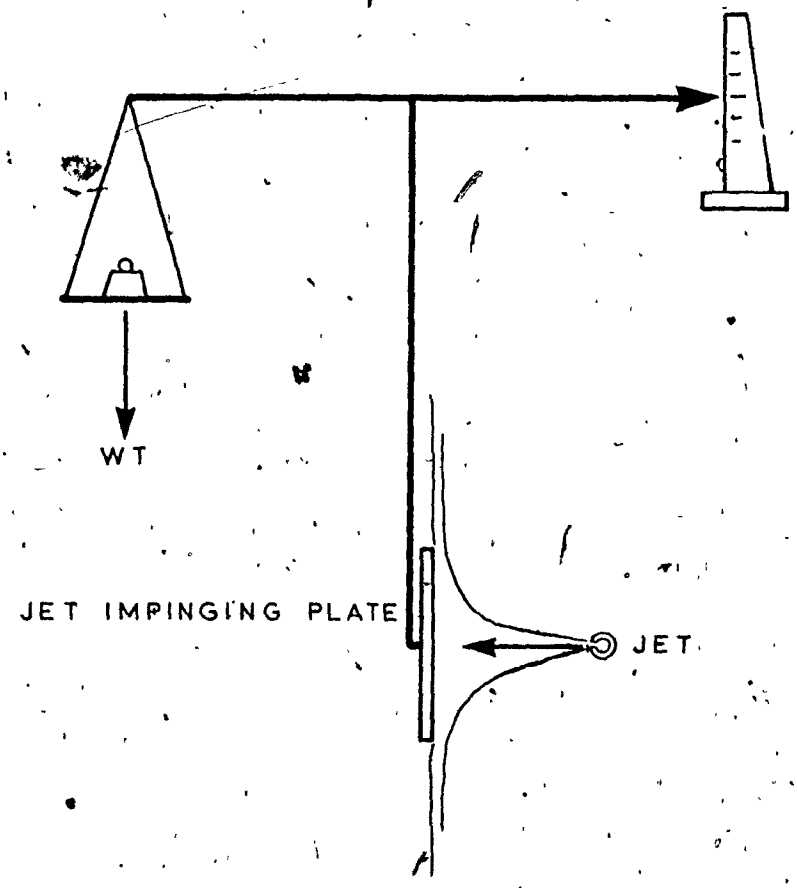

FIG. 4
MOMENTUM BALANCE

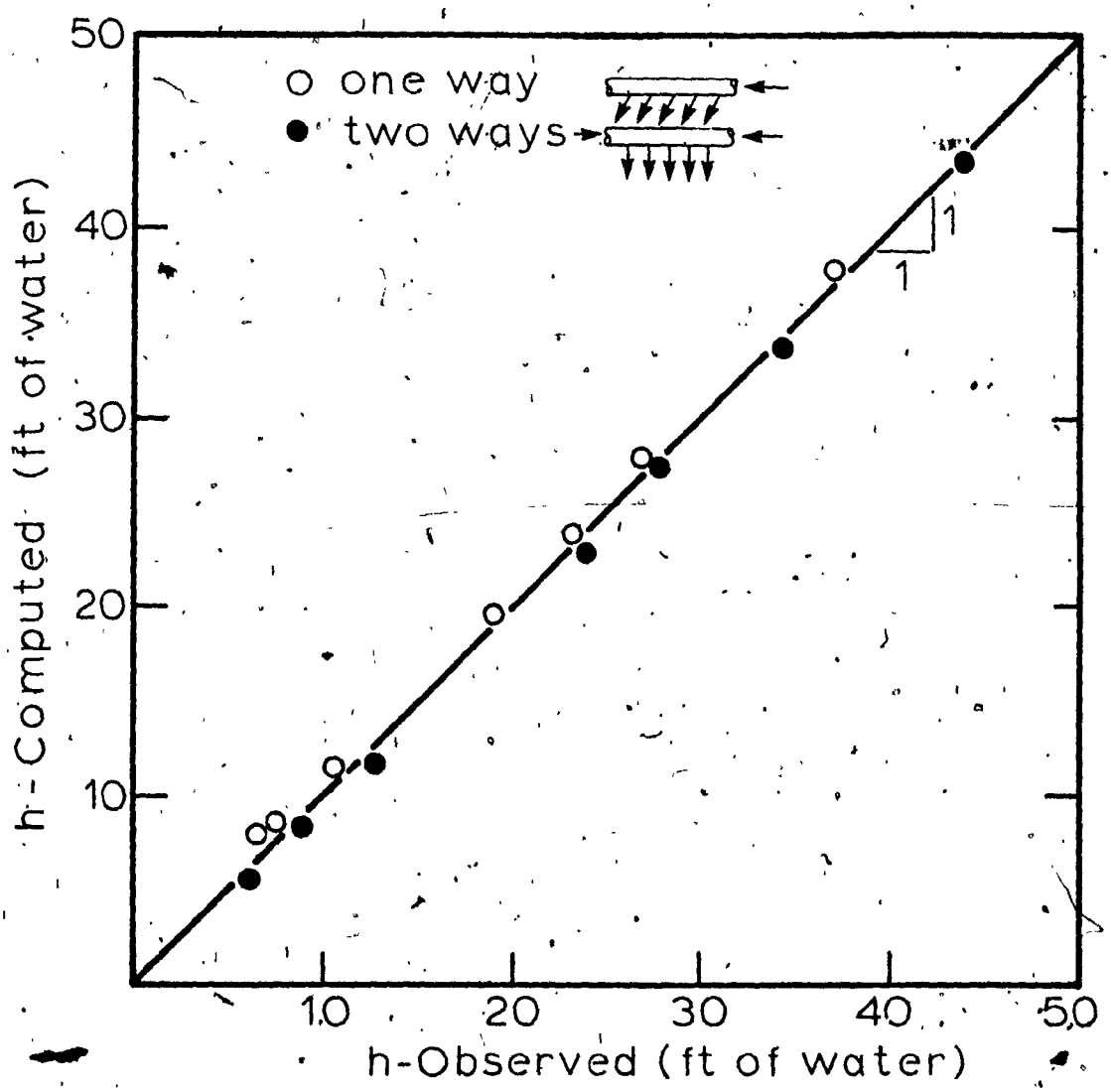

FIG. 5.
h-COMPUTED vs h-OBSERVED

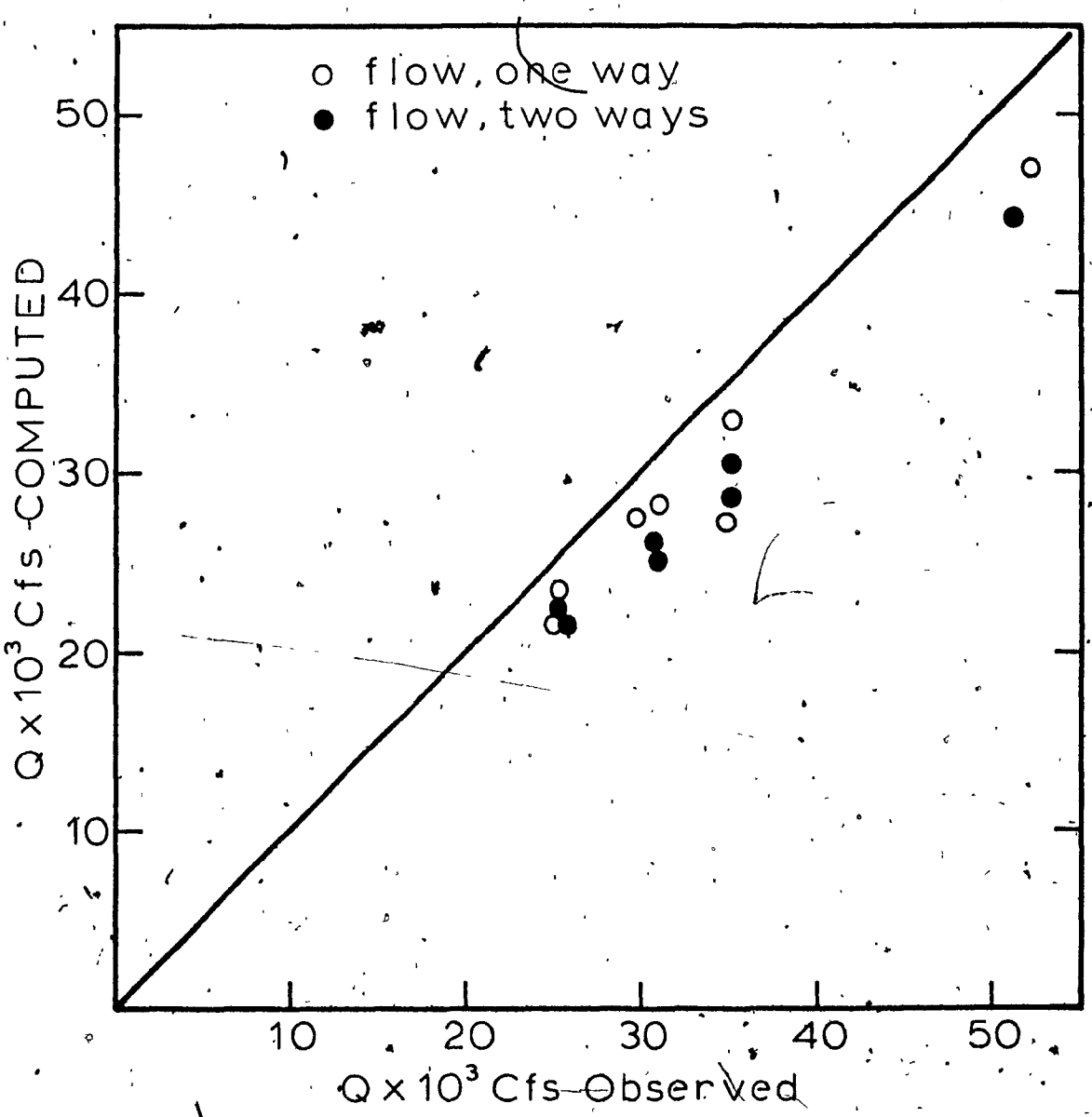

FIG. 6
Q COMPUTED vs Q OBSERVED

FIG. 7
MOMENTUM MEASURED BY USING BALANCE VERSUS MOMENTUM MEASURED BY USING PITOT TUBE

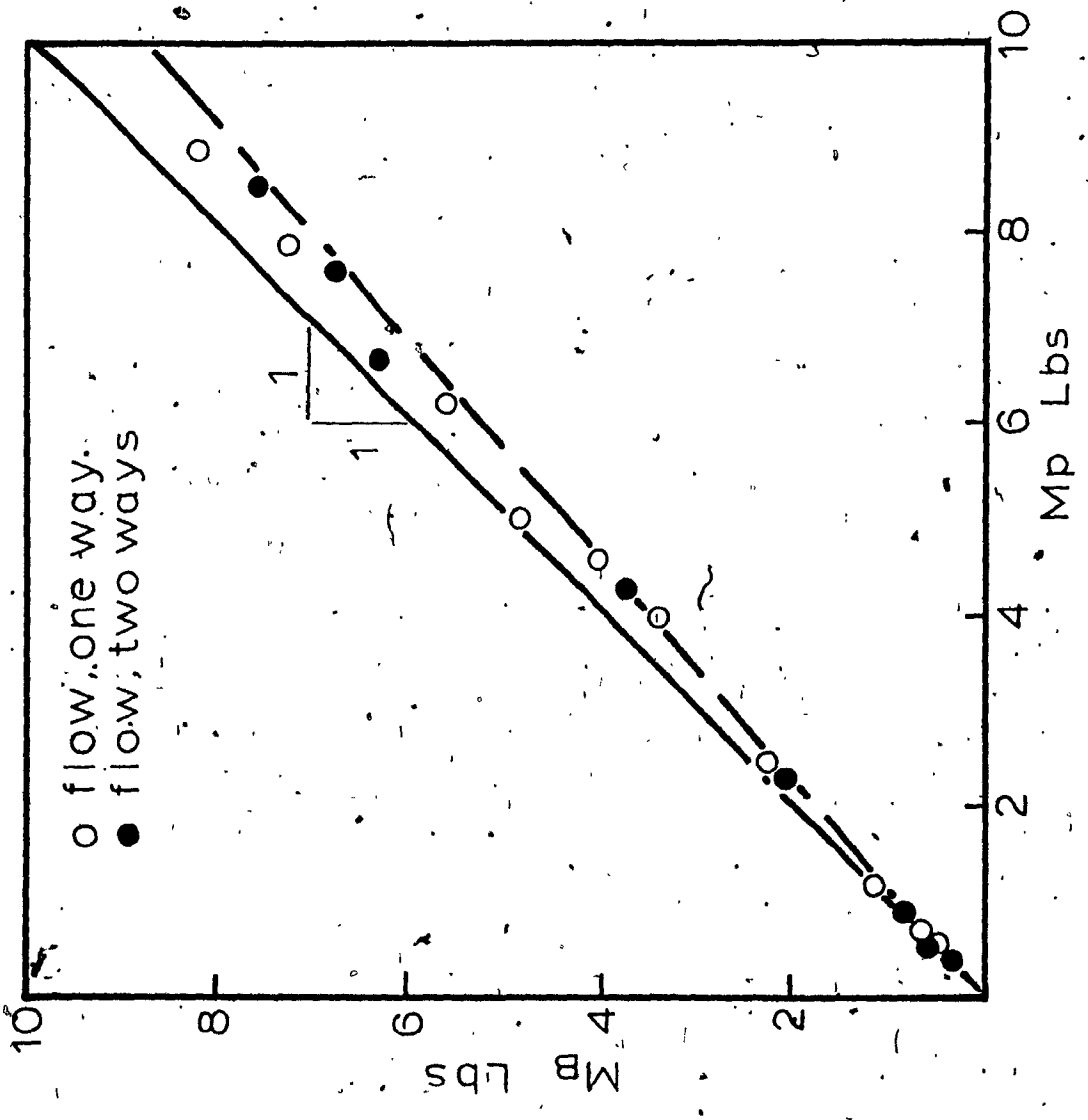

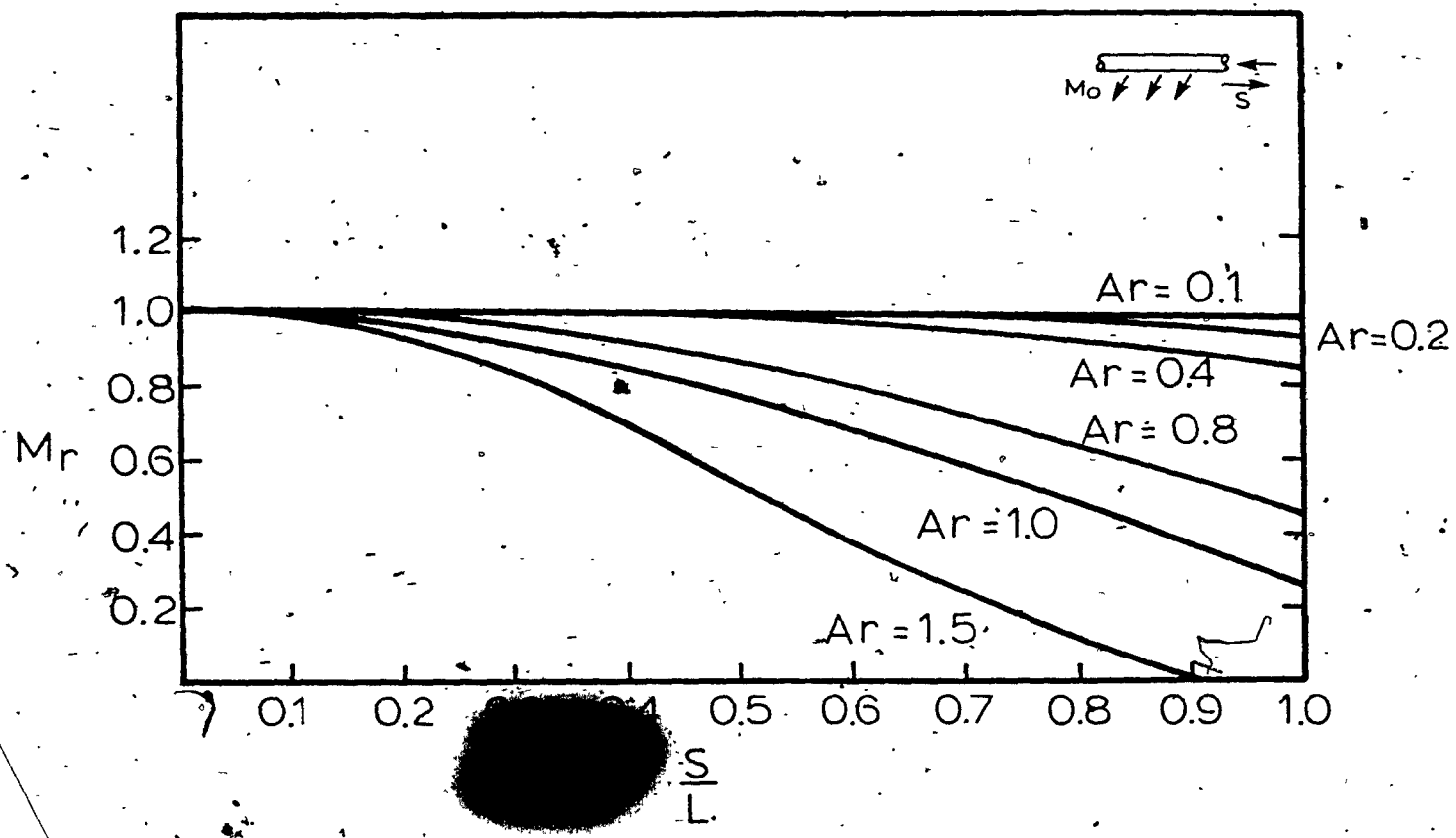

FIG. 8
THEORETICAL MOMENTUM DISTRIBUTION

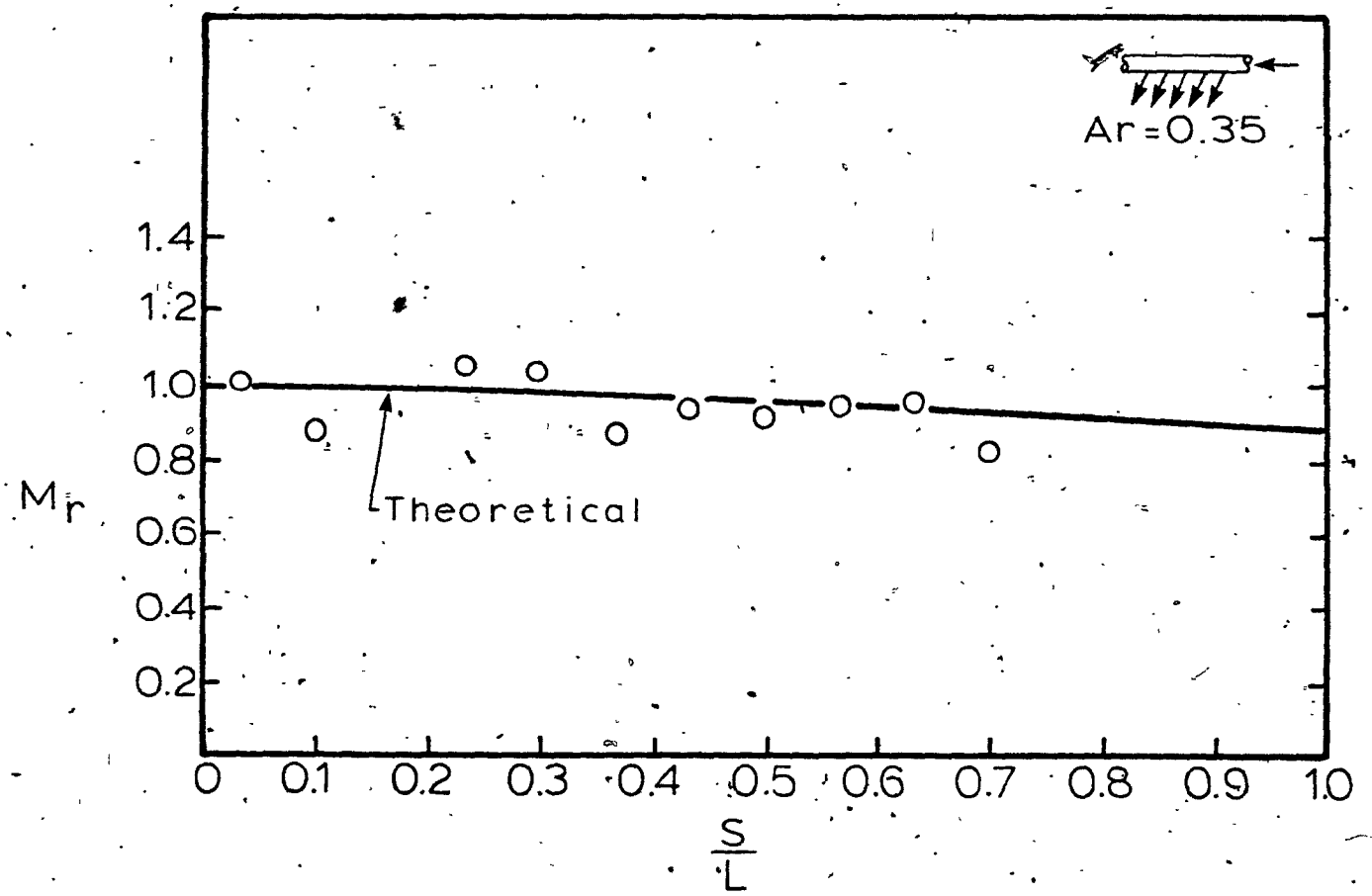

FIG. 9
MOMENTUM DISTRIBUTION

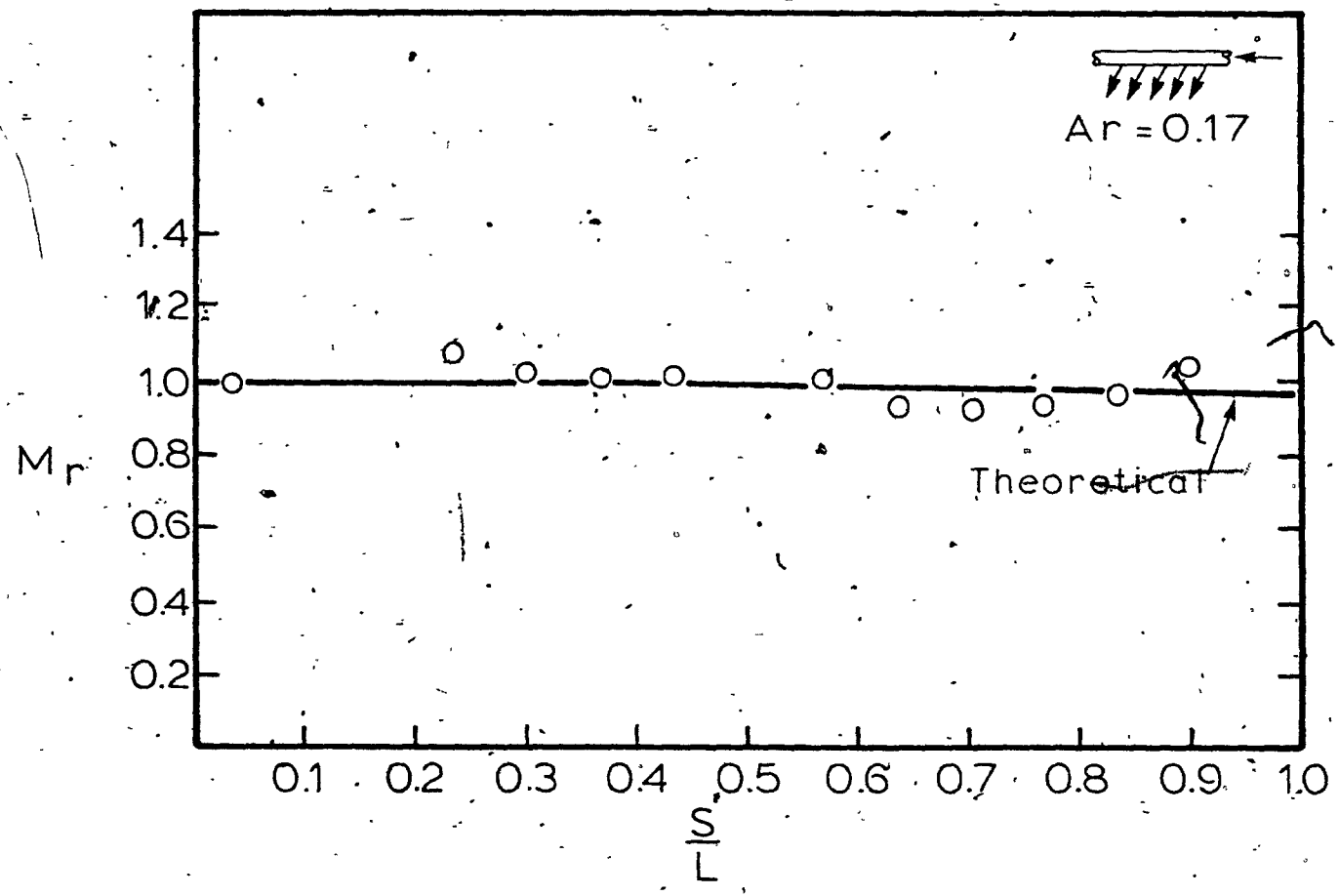

FIG. 10
MOMENTUM DISTRIBUTION

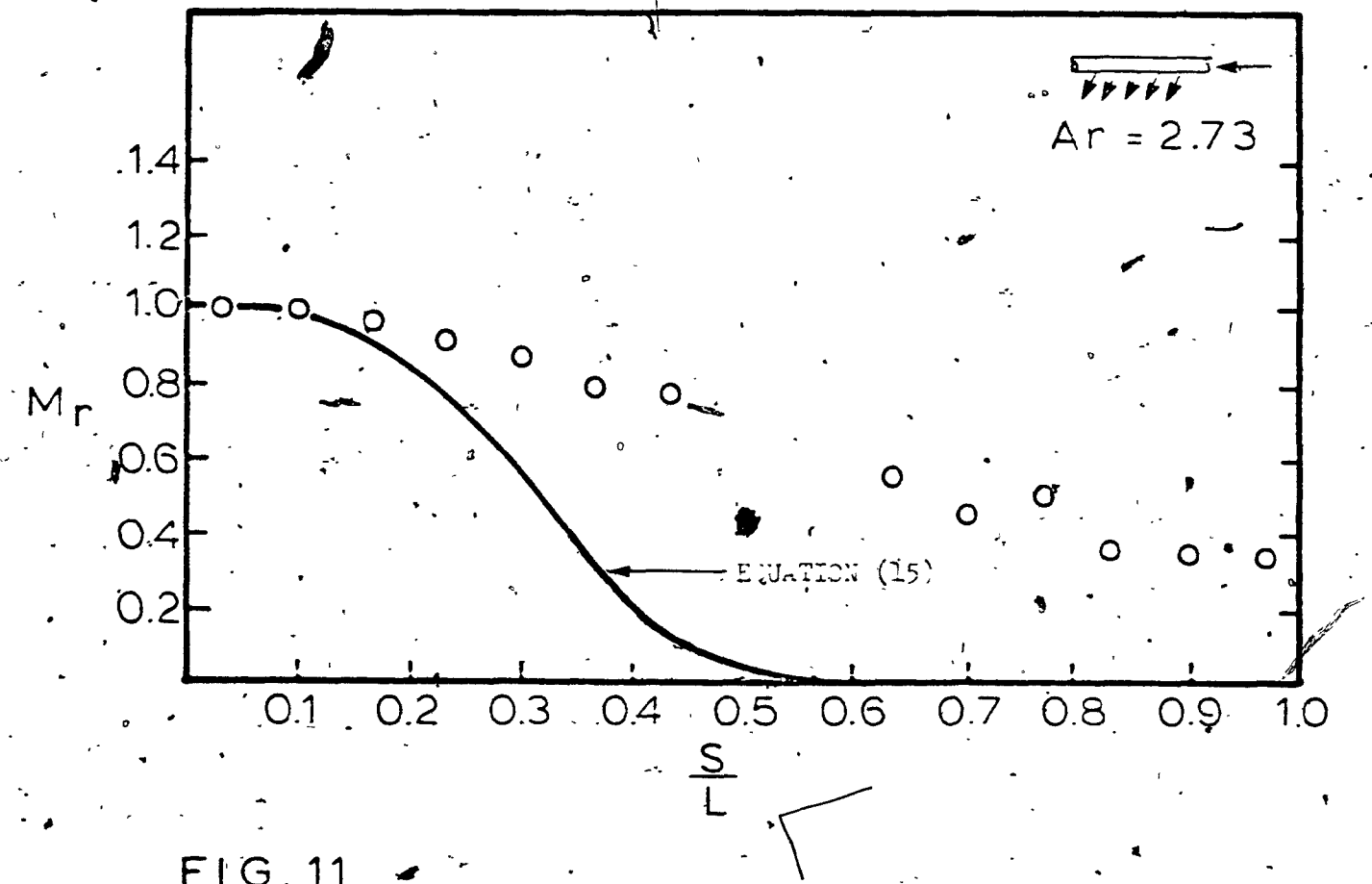

FIG. 11
MOMENTUM DISTRIBUTION.

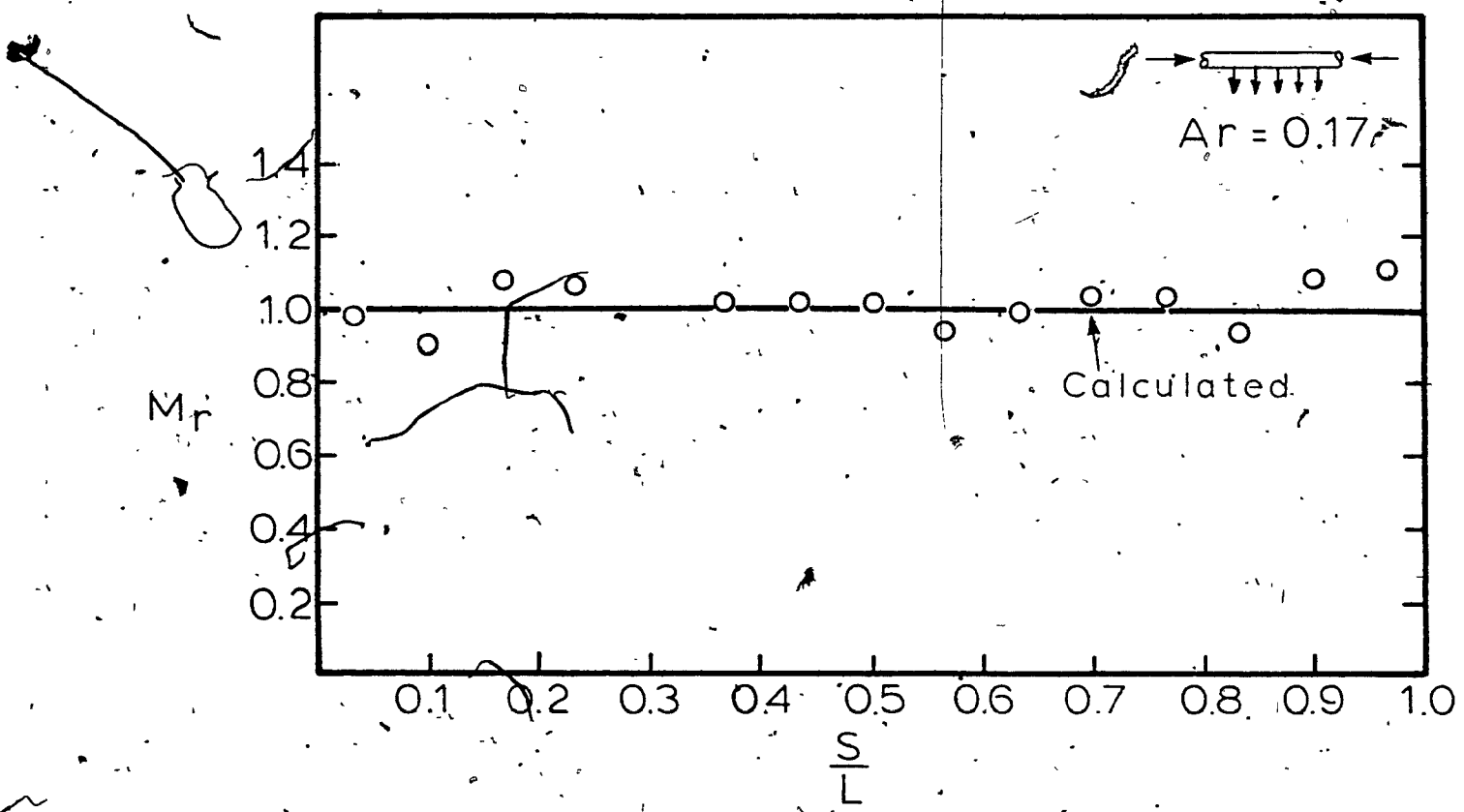

FIG. 12
MOMENTUM DISTRIBUTION

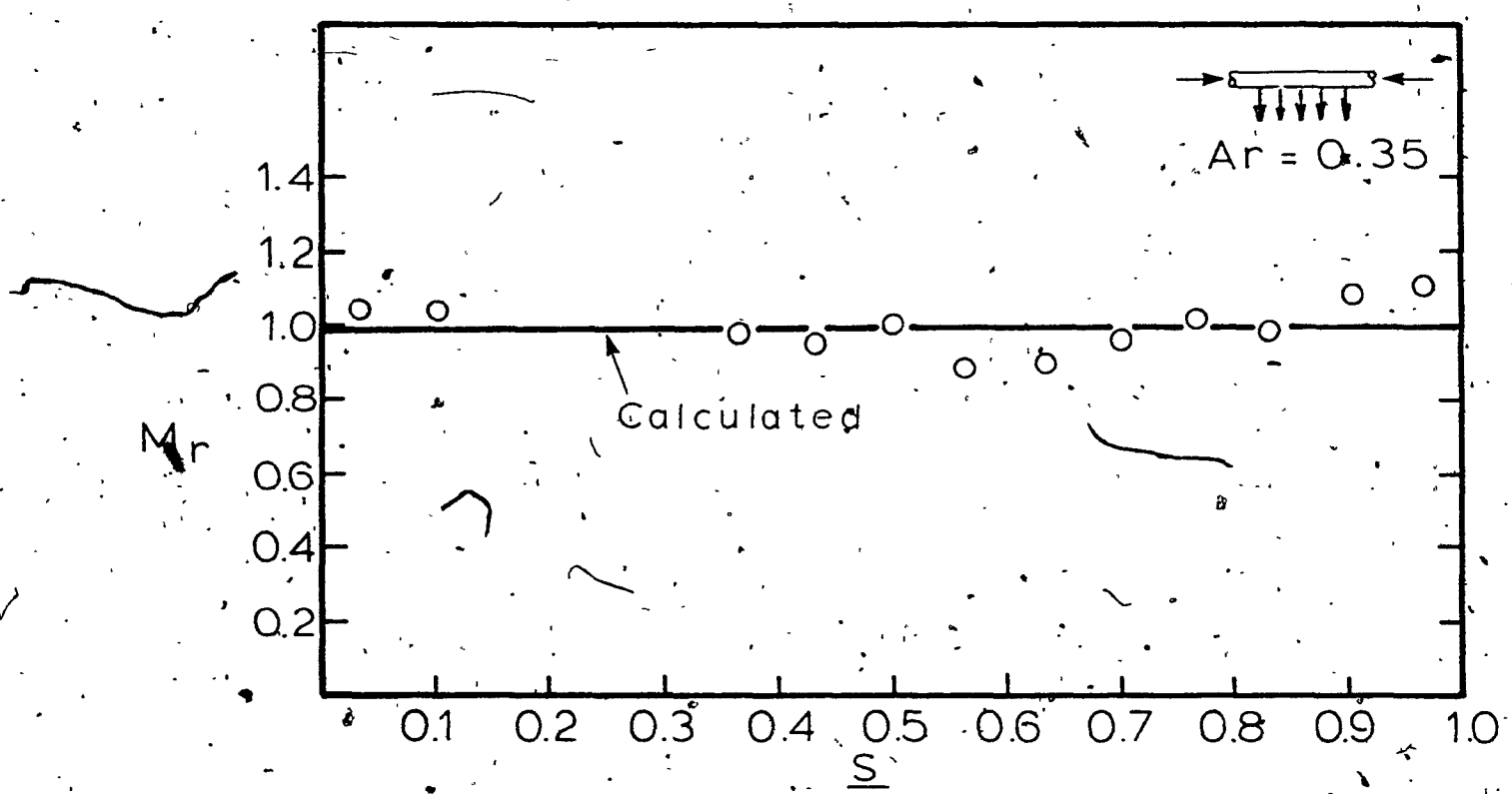

FIG. 13
MOMENTUM DISTRIBUTION

APPENDIX - A

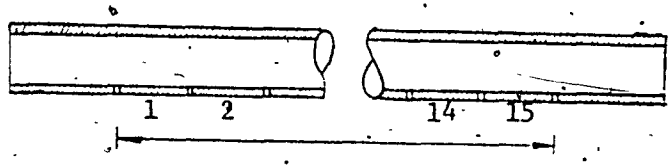

16 holes at 1.33 in.= 20 in.

RUN NO. 9 DATE=JAN 28 TUBE SIZE= .5

D	DIST	S	Q
.313	.782	.125	.157

LEVEL 4

2	3	4	5	6	7	8	9	10	11	12	13	14	15
1.563	1.560	1.560	1.562	1.562	1.560	1.560	1.560	1.560	1.560	1.560	1.560	1.560	1.560
1.562	1.562	1.562	1.562	1.561	1.560	1.562	1.560	1.560	1.560	1.560	1.560	1.562	1.560
1.582	2.322	2.262	2.328	2.886	2.820	2.520	2.760	2.400	1.960	1.880	1.920	1.740	1.780
1.660	3.447	3.102	3.228	3.264	3.240	3.022	2.100	3.420	2.420	2.360	2.320	2.082	2.080
1.660	3.120	3.240	2.928	2.784	2.886	2.582	1.824	3.023	2.100	2.040	2.060	1.980	1.940
1.600	2.100	2.360	2.220	2.220	1.960	2.002	1.788	2.328	2.200	1.940	2.060	1.882	1.820
1.560	1.920	1.660	1.752	1.660	1.660	1.620	1.680	1.822	1.660	1.920	1.960	1.720	1.740
1.560	1.580	1.580	1.640	1.580	1.580	1.620	1.600	1.560	1.640	1.640	1.620	1.640	1.582
1.562	1.562	1.560	1.562	1.560	1.560	1.560	1.560	1.560	1.562	1.560	1.560	1.560	1.560
1.560	1.560	1.560	1.560	1.562	1.560	1.560	1.560	1.560	1.560	1.560	1.560	1.560	1.560
1.560	1.560	1.560	1.560	1.560	1.560	1.560	1.560	1.560	1.560	1.560	1.560	1.560	1.560
1.560	1.560	1.560	1.560	1.560	1.560	1.560	1.560	1.560	1.560	1.560	1.560	1.560	1.560

VELOCITY DISTRIBUTION

0.000	0.000	0.000	0.000	0.000	0.000	0.000	0.000	0.000	0.000	0.000	0.000	0.000	0.000
0.000	0.000	0.000	0.000	0.000	0.000	0.000	0.000	0.000	0.000	0.000	0.000	0.000	0.000
.508	3.129	3.003	3.129	3.756	4.008	3.510	2.506	3.882	2.256	2.130	1.943	1.523	1.693
1.243	4.921	4.454	4.644	4.579	4.652	4.336	2.760	4.849	3.328	3.213	3.129	2.568	2.637
1.135	4.454	4.596	4.185	3.964	3.798	3.625	1.830	4.336	2.887	2.868	2.868	2.512	2.553
.879	2.723	3.213	2.671	2.565	2.272	2.361	1.663	3.129	2.971	2.212	2.638	2.153	2.032
.506	2.153	1.965	1.645	1.243	.718	.879	.718	1.832	1.980	2.093	2.003	1.436	1.523
2.000	.508	.632	.718	.718	.506	.879	.718	.508	1.715	.718	.879	1.215	.508
0.000	0.000	0.000	0.000	0.000	0.000	0.000	0.000	0.000	0.000	0.000	0.000	0.000	0.000
0.000	0.000	0.000	0.000	0.000	0.000	0.000	0.000	0.000	0.000	0.000	0.000	0.000	0.000
0.000	0.000	0.000	0.000	0.000	0.000	0.000	0.000	0.000	0.000	0.000	0.000	0.000	0.000
0.000	0.000	0.000	0.000	0.000	0.000	0.000	0.000	0.000	0.000	0.000	0.000	0.000	0.000

VELOCITY SQUARE DISTRIBUTION

0.000	0.000	0.000	0.000	0.000	0.000	0.000	0.000	0.000	0.000	0.000	0.000	0.000	0.000
0.000	0.000	0.000	0.000	0.000	0.000	0.000	0.000	0.000	0.000	0.000	0.000	0.000	0.000
.258	9.789	9.016	9.789	14.436	16.229	12.365	6.698	11.850	5.152	4.122	4.379	2.318	2.834
1.546	24.214	19.835	21.381	21.395	21.638	19.845	7.724	23.057	11.777	10.314	9.789	6.698	6.955
1.288	19.835	21.123	17.517	15.714	14.425	13.138	3.349	18.805	6.955	5.667	6.698	5.412	4.894
.773	7.470	10.301	8.243	6.698	5.152	5.667	2.834	9.789	8.243	4.894	4.440	4.637	4.122
.258	4.437	3.866	2.575	1.546	.515	.773	.515	3.349	3.864	4.379	4.379	2.061	2.318
0.000	.258	.258	.515	.258	.258	.773	.515	.258	1.030	.515	.773	1.030	.258
0.000	0.000	0.000	0.000	0.000	0.000	0.000	0.000	0.000	0.000	0.000	0.000	0.000	0.000
0.000	0.000	0.000	0.000	0.000	0.000	0.000	0.000	0.000	0.000	0.000	0.000	0.000	0.000
0.000	0.000	0.000	0.000	0.000	0.000	0.000	0.000	0.000	0.000	0.000	0.000	0.000	0.000
0.000	0.000	0.000	0.000	0.000	0.000	0.000	0.000	0.000	0.000	0.000	0.000	0.000	0.000

MOMENTUM DISTRIBUTION

.264	.269	.267	.263	.263	.261	.254	.223	.271	.238	.231	.234	.223	.221	.221

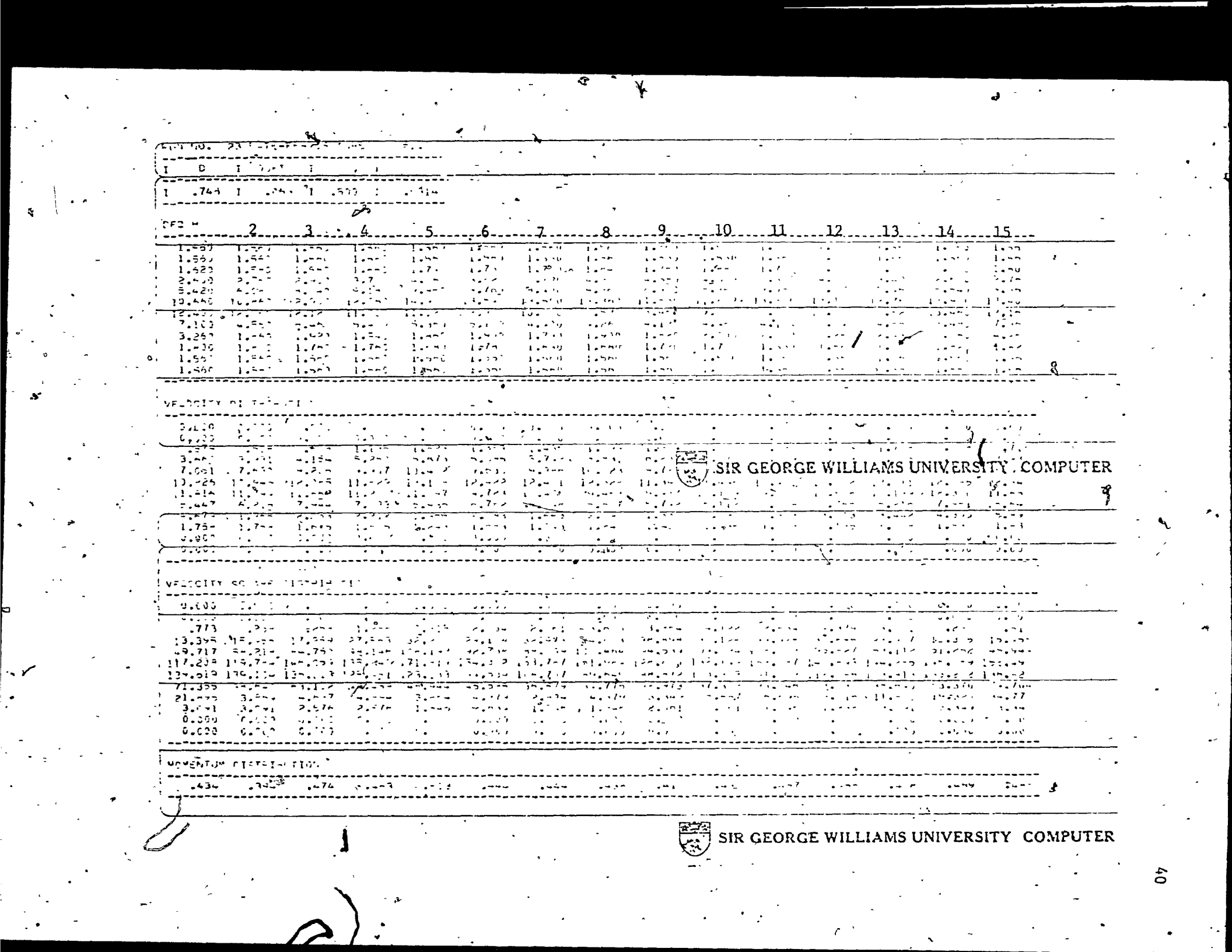

SIR GEORGE WILLIAMS UNIVERSITY COMPUTER

SIR GEORGE WILLIAMS UNIVERSITY COMPUTER

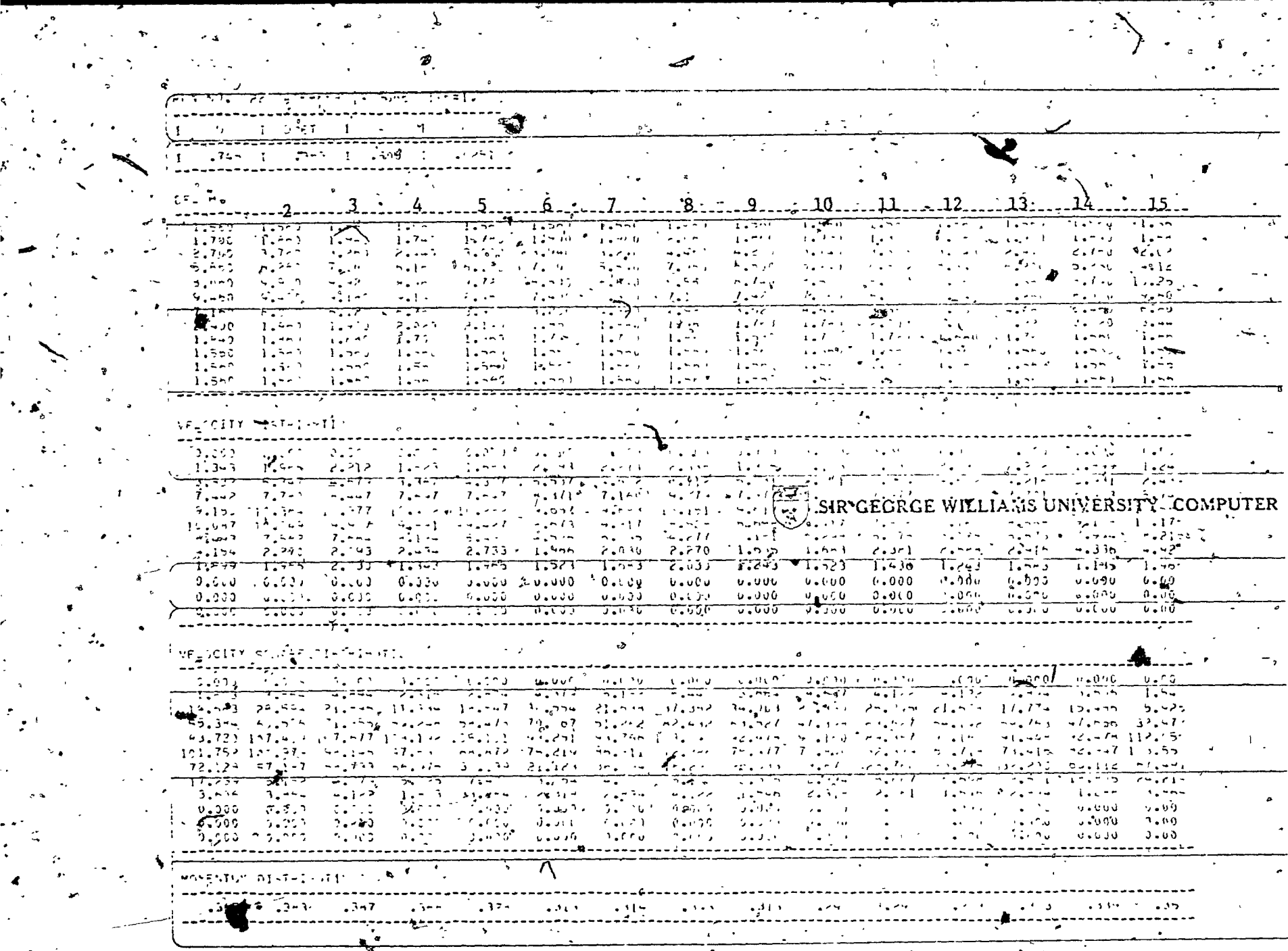

SIR GEORGE WILLIAMS UNIVERSITY COMPUTER

SIR GEORGE WILLIAMS UNIVERSITY COMPUTER

RUN NO. 21 DATE=FEB 64 TUBE SIZE=1.0

I D	I DIFT	I S	I Q
I .748	I .363	I .500	I .0251

DEL R	2	3	4	5	6	7	8	9	10	11	12	13	14	15
1.560	1.560	1.562	1.560	1.560	1.560	1.560	1.560	1.560	1.560	1.560	1.560	1.560	1.562	1.560
1.560	1.608	1.608	1.560	1.560	1.560	1.560	1.560	1.560	1.560	1.608	1.560	1.560	1.560	1.608
3.528	4.223	4.680	3.960	3.460	3.060	2.480	3.520	2.880	2.928	2.976	3.168	2.928	2.928	2.880
5.368	5.232	6.820	7.720	7.120	7.140	5.960	8.600	6.320	5.660	6.028	7.320	6.480	6.360	5.660
8.920	9.760	11.120	11.560	11.600	9.400	9.260	9.000	8.320	8.460	9.060	9.220	8.920	9.200	9.160
8.960	8.620	8.860	13.220	13.180	7.860	9.060	6.880	7.160	8.200	8.180	7.960	8.140	8.560	9.420
6.020	5.380	5.200	4.460	4.860	3.820	3.860	3.820	4.060	4.200	4.460	4.820	5.060	6.760	7.480
2.260	2.240	1.920	1.960	2.080	2.000	1.960	1.980	2.280	1.940	2.040	1.920	1.980	2.160	2.260
1.520	1.560	1.560	1.560	1.560	1.600	1.560	1.600	1.600	1.560	1.560	1.600	1.600	1.560	1.560
1.560	1.560	1.560	1.560	1.560	1.560	1.560	1.560	1.560	1.560	1.560	1.560	1.560	1.560	1.560
1.560	1.560	1.560	1.560	1.560	1.560	1.560	1.560	1.560	1.560	1.560	1.560	1.560	1.560	1.560
1.560	1.560	1.560	1.560	1.560	1.560	1.560	1.560	1.560	1.560	1.560	1.560	1.560	1.560	1.560

VELOCITY DISTRIBUTION

0.000	0.000	0.000	0.000	0.000	0.000	0.000	0.000	0.000	0.000	0.000	0.000	0.000	0.000	0.000
.576	.718	.718	.508	.508	.508	.508	0.000	0.000	.508	.718	.508	.508	.508	0.000
4.999	5.803	6.339	5.443	4.947	4.395	3.442	5.024	4.104	4.185	4.154	4.511	4.165	4.154	3.992
6.995	6.847	8.215	8.907	8.447	8.476	7.528	9.522	7.830	7.267	7.662	8.598	7.661	7.862	7.[illegible]
9.736	12.277	11.997	11.368	11.372	13.049	9.959	9.789	9.334	9.[illegible]	9.[illegible]	9.[illegible]	9.[illegible]	9.[illegible]	9.[illegible]
9.763	9.536	9.697	13.561	10.468	9.008	9.629	8.215	8.493	9.108	9.178	9.079	9.206	9.495	10.249
7.579	6.714	6.656	6.112	6.523	5.371	5.443	5.395	5.675	5.831	6.112	6.480	6.714	8.184	8.673
3.223	2.496	2.153	2.326	2.538	2.361	2.326	2.326	2.988	2.212	2.486	2.153	2.326	2.751	3.223
.679	.508	.508	.508	.508	.718	.508	.718	.718	.508	.508	.718	.718	.508	.508
0.000	0.000	0.000	0.000	0.000	0.000	0.000	0.000	0.000	0.000	0.000	0.000	0.000	0.000	0.000
0.000	0.000	0.000	0.000	0.000	0.000	0.000	0.000	0.000	0.000	0.000	0.000	0.000	0.000	0.000
0.000	0.000	0.000	0.000	0.000	0.000	0.000	0.000	0.000	0.000	0.000	0.000	0.000	0.000	0.000

VELOCITY SQUARE DISTRIBUTION

0.000	0.000	0.000	0.000	0.000	0.000	0.000	0.000	0.000	0.000	0.000	0.000	0.000	0.000	0.000
.258	.515	.515	.258	.258	.258	.258	0.000	0.000	.258	.515	.258	.258	.258	.773
24.987	34.261	43.106	29.624	24.472	19.320	11.852	25.246	17.302	17.517	17.259	20.359	17.517	17.259	15.744
48.944	46.893	67.491	79.341	71.355	71.870	56.672	98.675	61.319	52.208	57.187	73.931	63.379	61.824	52.894
94.797	105.616	123.133	129.258	129.315	103.979	99.176	95.827	87.269	88.972	96.602	98.661	94.797	95.827	97.888
95.312	98.933	94.424	111.541	109.995	81.144	96.602	67.491	72.128	82.947	84.235	82.432	84.750	98.161	107.970
57.445	45.393	44.307	37.352	42.504	28.851	29.624	29.129	32.200	34.003	37.352	41.989	45.080	66.026	75.219
9.316	6.182	4.637	5.410	6.698	5.607	5.410	5.410	6.598	4.894	6.182	4.637	5.410	7.728	9.316
.773	.258	.258	.258	.258	.515	.258	.515	.515	.258	.515	.515	0.000	.258	.258
0.000	0.000	0.000	0.000	0.000	0.000	0.000	0.000	0.000	0.000	0.000	0.000	0.000	0.000	0.000
0.000	0.000	0.000	0.000	0.000	0.000	0.000	0.000	0.000	0.000	0.000	0.000	0.000	0.000	0.000
0.000	0.000	0.000	0.000	0.000	0.000	0.000	0.000	0.000	0.000	0.000	0.000	0.000	0.000	0.000

MOMENTUM DISTRIBUTION

.345	.343	.397	.489	.481	.321	.312	.327	.288	.293	.312	.336	.325	.354	.369

RUN NO. 15 DATE-JAN 24 TUBE SIZE=1.0

I	D	I	DJET	I	S	I	Q
I	.748	I	.363	I	.250	I	.0251

DEL H	2	3	4	5	6	7	8	9	10	11	12	13	14	15
1.560	1.560	1.560	1.560	1.560	1.560	1.560	1.560	1.560	1.560	1.560	1.560	1.560	1.560	1.560
1.760	1.720	1.680	1.680	1.700	1.640	1.640	1.660	1.640	1.680	1.720	1.720	1.720	2.660	1.640
1.820	1.820	1.840	1.900	1.800	1.760	1.700	1.680	1.720	1.740	1.960	1.720	1.760	1.820	1.920
2.820	2.580	2.520	2.800	2.320	1.920	1.840	2.100	2.240	2.360	2.480	2.220	2.260	2.380	2.320
3.540	3.540	3.820	3.520	3.720	3.220	2.680	3.200	3.360	3.620	3.620	3.760	3.780	3.740	3.920
4.300	4.480	5.440	5.200	5.360	4.660	3.920	4.320	4.460	4.200	3.920	5.600	5.360	5.220	5.120
5.000	3.620	5.000	3.920	3.960	5.200	4.660	4.720	4.920	4.180	3.360	5.520	5.060	4.800	4.820
2.720	2.640	3.000	3.480	3.320	3.400	3.420	2.980	2.480	2.980	2.520	3.820	3.720	4.160	4.800
1.960	2.000	2.000	2.360	2.160	2.720	2.560	2.460	2.120	2.420	2.120	2.320	3.320	3.460	3.320
1.760	1.720	1.680	1.680	1.700	1.640	1.640	1.660	1.640	1.680	1.700	1.720	1.720	2.660	1.640
1.560	1.560	1.560	1.560	1.560	1.560	1.560	1.560	1.560	1.560	1.560	1.560	1.560	1.560	1.560
1.560	1.560	1.560	1.560	1.560	1.560	1.560	1.560	1.560	1.560	1.560	1.560	1.560	1.560	1.560

VELOCITY DISTRIBUTION

0.000	0.000	0.000	0.000	0.000	0.000	0.000	0.000	0.000	0.000	0.000	0.000	0.000	0.000	0.000
1.605	1.436	1.243	1.243	1.343	1.015	1.015	1.135	1.015	1.243	1.343	1.343	1.436	3.764	1.015
1.758	1.758	1.899	2.093	1.758	1.605	1.343	1.243	1.436	1.523	2.278	1.436	1.605	1.830	2.153
4.028	3.626	3.516	3.996	3.129	2.093	1.899	2.637	2.959	3.218	3.442	2.871	3.003	3.250	3.787
5.050	5.050	5.395	5.724	5.250	4.624	3.798	4.596	4.815	5.151	5.151	5.323	5.347	5.299	5.491
5.941	6.133	7.033	6.847	6.996	6.319	5.513	5.962	6.112	5.931	5.513	7.214	6.987	6.847	6.752
6.666	5.151	6.655	5.513	5.560	6.847	6.319	6.383	6.579	5.809	4.815	7.124	6.714	5.467	6.491
3.865	3.719	4.317	4.973	4.761	4.866	4.895	4.277	3.442	4.277	3.480	5.395	5.275	5.787	5.403
2.272	2.391	2.351	2.538	2.788	3.865	3.509	3.405	2.686	3.328	2.686	3.129	4.761	4.947	4.761
1.605	1.436	1.243	1.243	1.343	1.015	1.015	1.135	1.015	1.243	1.343	1.343	1.436	3.764	1.015
0.000	0.000	0.000	0.000	0.000	0.000	0.000	0.000	0.000	0.000	0.000	0.000	0.000	0.000	0.000
0.000	0.000	0.000	0.000	0.000	0.000	0.000	0.000	0.000	0.000	0.000	0.000	0.000	0.000	0.000

VELOCITY SQUARE DISTRIBUTION

0.000	0.000	0.000	0.000	0.000	0.000	0.000	0.000	0.000	0.000	0.000	0.000	0.000	0.000	0.000
2.576	2.761	1.546	1.546	1.803	1.030	1.030	1.288	1.030	1.546	1.803	1.803	2.761	14.168	1.030
3.091	3.091	3.606	4.379	3.391	2.576	1.803	1.546	2.761	2.318	5.152	2.761	2.576	3.349	4.637
16.229	13.139	12.365	15.971	9.789	4.379	3.606	6.955	8.758	13.384	11.850	8.243	9.016	10.552	9.531
25.592	25.592	29.189	25.245	27.563	21.381	14.426	21.123	23.184	26.533	26.533	28.336	28.594	28.078	30.139
35.291	37.618	49.459	46.883	48.944	39.928	30.397	35.549	37.352	34.003	30.397	52.735	48.815	46.883	45.595
44.327	26.533	44.327	32.397	30.912	46.883	39.928	40.721	43.277	33.746	23.184	50.747	45.080	41.731	41.989
14.941	13.912	18.547	24.732	22.669	23.699	23.957	18.298	11.850	18.298	12.107	29.149	27.821	33.488	41.731
5.152	5.667	5.667	6.440	7.728	14.941	12.880	11.592	7.213	11.277	7.213	9.789	22.669	24.472	22.569
2.576	2.761	1.546	1.546	1.803	1.030	1.030	1.288	1.030	1.546	1.803	1.803	2.761	14.168	1.030
0.000	0.000	0.000	0.000	0.000	0.000	0.000	0.000	0.000	0.000	0.000	0.000	0.000	0.000	0.000
0.000	0.000	0.000	0.000	0.000	0.000	0.000	0.000	0.000	0.000	0.000	0.000	0.000	0.000	0.000

MOMENTUM DISTRIBUTION

.156	.135	.173	.164	.161	.162	.134	.144	.141	.145	.125	.192	.197	.226	.227

APPENDIX B

SPECIMEN CALCULATION

Appendix B

A) Calculation of pressure P_3 at entrance to the manifold using gauge pressure P_1 (observed).

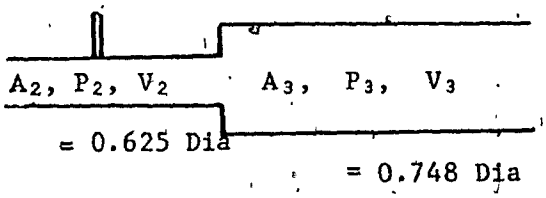

Figure B_1

The following relation holds for Figure B_1

$$\frac{P_2}{\gamma} + \frac{V_2^2}{2g} = \frac{P_3}{\gamma} + \frac{V_3^2}{2g} + \frac{(V_2 - V_2)^2}{2g} \qquad (17)$$

and $$Q = V_2 A_2 = V_3 A_3 \qquad (18)$$

Data

$Q = 0.0251$ cfs $\therefore V_2 = 11.95$ ft/sec. $V_3 = 8.1$ ft/sec.

$\frac{P_1}{\gamma} = 5.71$ ft.

using the above relation, one gets

$$5.71 + \frac{11.95^2}{2 \times 32.2} = \frac{P_2}{\gamma} + \frac{8_1^2}{2 \times 32.2} + \frac{(11.95 - 8.1)^2}{2 \times 32.2}$$

$$\frac{P_2}{\gamma} = 6.68 \text{ ft.}$$

B) Computation of h. Theoretical

For a set of conditions given below h can be calculated as follows:

The following equation from Chapter III is used.

$$\frac{h}{H} = \cos^2 \left(\frac{\mu a}{A} S\right)$$

$\mu = 0.61$ $S = 1.33$ ft. $\frac{a}{A} = 3.5$ $H = 7.7$ ft.

$h = 6.81$ ft.

c) Theoretical Discharge Calculation

Theoretical discharge is calculated using the following relationship given in Chapter V.

$$Q = A \frac{\sqrt{2gH}}{\alpha} \sin \left(\frac{\mu a}{A} L\right) \qquad (16)$$

$A = 0.0305$ sq.ft. $H = 7.7$ ft $\mu = 0.61$

$\frac{a}{A} = 0.35$ $L = 1.77$ ft.

$Q = 23.1$ cfs.

References

(1) Giorgio Noseda, "Experimental study on pipes with rate of flow decreasing along their length," I.A.H.R. General Meeting Transaction, 2 (1957), D 8-1 to D 8-9.

(2) J. D. Keller, "The Manifold Problems", A.S.M.E. Transactions, 71 (1956), 77-85.

(3) J. A. B. Albinson, "An investigation of the manifold problem for imcompressible fluids with special reference to the use of manifolds for canal locks," Proc. Institute of Engineers, V, 4 (1955), 114-138.

(4) F. C. W. Olson, "Flow through a pipe with a porous wall," Journal of Applied Mechanics, Transactions A.S.M.E., 71 (1949), 53-54 and (Sept.), 317-318.

(5) S. Vigander, R. E. Elder, and N. H. Brooks, "Internal hydraulics of thermal discharge difference," A.S.C.E. Hydraulics Division, 96 (1970), 509-527.

(6) J. Berlamont and A. Vander Beken, "Solution for lateral end flow in perforated conditions," A.S.C.E. Hydraulics Division, 99 (1973), 1531-1549.

(7) Lin, Blockage characteristics of plane counter jet (July, 1973). Master of Engineering Thesis, S.G.W.U.

(8) Enger & Levy, "Pressure in Manifold Pipes," Journal American Water Works Assoc., 21 (May, 1929), 659-667.

(9) W. M. Dow, "The uniform distribution of fluid flowing through a perforated pipe," Journal of Applied Mechanics, 17, No. 4 (1950), 431-438.

(10) Z. Van der Hegge, "Flow through uniformly tapped pipe," Applied Scientific Research, A3, No. 2 (1951), 144-162.

(11) W. E. Howland, "Design of perforated pipe to uniform in discharge," Proceedings of Third Mid Western Conference on Fluid Mechanics, 1953, pp. 687-701.

(12) J. H. Horlock, "An investigation of flow in manifolds with open and closed ends," Journal of the Royal Aeronautical Society, 60 (1956), 749-753.

(13) A. Arcrivos, "Flow Distribution in manifolds," Chemical Engineering Science, 10 (1959), 112-124.

(14) E. Markland, "The analysis of flow from pipe manifolds," Engineering 187, No. 4847 (1959), 150-151.

(15) Steel & Shove, "Design chart for flow and pressure distribution in perforated air ducts," Transactions ASAE, 12, No. 2 (1969), 220-224.

(16) T. R. Camp and S. D. Graber, Discussion of Internal Hydraulics Division ASCE, 96, No. Hy12, proc. paper 5871 (1968), 31-39.

(17) E. Zsak, "Manifold flow in subirrigation pipes," Journal of Hydraulics Division ASCE, 97, No. Hy10, paper 8477 (Oct. 1971), 1737-1746.